

Noise analysis for the ion trap implementation of the quantum Rabi model in the deep strong coupling regime

Ricardo Puebla, Jorge Casanova and Martin B. Plenio

Institut für Theoretische Physik and IQST,

Albert-Einstein-Allee 11, Universität Ulm, D-89069 Ulm, Germany

Abstract

The dynamics of the quantum Rabi model in the deep strong coupling regime is investigated in a trapped-ion setup. Recognizably, the main hallmark of this regime is the emergence of collapses and revivals, whose faithful observation is hindered under realistic magnetic dephasing noise. Here we discuss how to attain a faithful implementation of the quantum Rabi model in the deep strong coupling regime which is robust against magnetic-field fluctuations and at the same time provides a large tunability of the simulated parameters. This is achieved by combining standing wave laser configuration with continuous dynamical decoupling. In this manner the present work further supports the suitability of continuous dynamical decoupling techniques in trapped-ion settings to faithfully realize different interacting dynamics.

I. INTRODUCTION

One of the simplest, yet fundamental, quantum models consists of a two-level system interacting with a single-mode bosonic field. This system, besides of being a nice textbook example of fundamental quantum physics, describes realistic phenomena in a variety of physical situations, and it is commonly known as quantum Rabi model (QRM), in honor of the groundbreaking work of the author of the same name who analyzed the interaction of a spin with a classical field [1, 2]. Certainly, this simple model emerges naturally in different physical situations; although primarily studied in the realm of quantum optics, its relevance encompasses even quantum information processing [3]. This underlies the considerable attention that this model has attracted and the efforts devoted during the last decades to elucidate the physics of the QRM [4]. Furthermore, although the first fully quantized version of this model dates from 1963 [5], the QRM still reveals new results, such as its integrability [6], the appearance of finite system quantum phase transition [7, 8] or the structured dynamics of revivals in the deep strong coupling (DSC) regime [9] to name a few recent insights.

However, the experimentally accessible parameter regime of the QRM is generally constrained to small couplings between the two subsystems (qubit and bosonic mode), hindering the observation of the rich phenomenology of the ultrastrong coupling regime. In this respect, recent works paved the way to scrutinize the ultrastrong coupling regime of the QRM, as in cavity QED [10, 11] or in a spin-mechanical system [12]. Among the diverse setups where the QRM is realized, trapped ions merit special attention as they combine qubits possessing long coherence time with high fidelity measurements [13, 14]. Furthermore, a quantum simulation of the QRM in a large variety of parameter regimes is possible in a trapped-ion setup [15], which enables the exploration of the DSC regime or the emergence of the quantum phase transition [16]. However, an accurate realization of the QRM crucially depends on the mitigation of the impact of different experimental imperfections into trapped-ion dynamics. We consider trapped-ion setups in which magnetic-field fluctuations constitute the main source of decoherence, as it is the case in typical experiments performed involving metastable state of optical ions [17, 18] or microwave-driven ions [19, 20]. Hence, the realization of a QRM with a trapped ion may be enhanced by means of schemes that are robust against these noise sources. In this context, the suitability of dynamical decoupling

(DD) techniques to simulate a QRM in a trapped ion setting has been recently reported by the authors in [21], and constitutes a promising tool to attain prolonged coherence times in setups mainly affected by magnetic-dephasing noise. However, the particular parameter regime of the QRM may not be trivially achieved with DD techniques due to either a breakdown of required approximations or the impossibility to have access to the desired parameters. Certainly, this fact challenges the achievement of a protected QRM in the DSC regime.

In this work we show that by combining continuous dynamical decoupling methods and standing wave configuration of the lasers to create interaction terms [22, 23], a magnetic-dephasing noise-resilient QRM can be accomplished even in the DSC regime. We illustrate the advantage of this scheme with respect to a bare realization by means of numerical simulations to observe the main hallmark of the QRM in this regime, namely, the emergence of collapses and revivals in the dynamics [9]. The article is organized as follows. We first introduce the QRM in Sec. II, and comment the physics of the DSC regime. Then, in Sec. III, we discuss how to realize a magnetic-dephasing noise resilient, yet tunable, QRM in a trapped-ion setup combining both continuous dynamical decoupling methods and standing wave configuration. Finally, in Sec. IV a summary of the main results is presented.

II. QUANTUM RABI MODEL

The QRM describes the interaction of a two-level system with a single-mode bosonic field. The Hamiltonian of this model can be written as

$$H_{\text{QRM}} = \frac{\omega}{2}\sigma_z + \omega_0 a^\dagger a - \lambda \sigma_x (a + a^\dagger), \quad (1)$$

where $\sigma_{x,y,z}$ are the Pauli operators acting on the two-level system, whose transition frequency is ω , and the usual creation and annihilation bosonic operators (a^\dagger and a) give account of the quantized single-mode bosonic field with frequency ω_0 . The subsystems interact through the last term of the Hamiltonian, with strength given by the coupling constant λ . It is worth mentioning that the Hamiltonian includes the so-called counter-rotating terms, namely, $\sigma^+ a^\dagger$ and $\sigma^- a$, which do not appear in the Jaynes-Cummings model (JC) [5]. As a consequence, the QRM does not conserve the total number excitations in the system, $N = a^\dagger a + \sigma^+ \sigma^-$. Nonetheless, the parity of N is conserved, namely this Z_2 parity symme-

try has an associated operator, $\Pi = -\sigma_z(-1)^{a^\dagger a}$, that commutes with the Hamiltonian and allows us to gain insight in its system dynamics [9].

In this work we focus in the DSC regime of the QRM. This regime takes place beyond the strong or ultrastrong coupling regimes [10, 11], that is, when the coupling constant becomes equal or larger than the bosonic frequency $\lambda/\omega_0 \gtrsim 1$ [9, 24]. The dynamics in this regime is characterized by collapses and revivals, which are periodically occurring in the solvable case $\omega = 0$ [9]. As demonstrated analytically in the latter case, an initial state $|\psi(0)\rangle$ evolves drawing periodic orbits in the phase space. Hence, $S(t) = |\langle\psi(0)|\psi(t)\rangle|^2$ reaches 1 at times $t_m = m2\pi/\omega_0$ with m a positive integer number, meaning that the initial state is perfectly retrieved. However, this situation slightly differs when considering a more general case, $\omega \neq 0$ but $\omega \sim \omega_0$, where despite the dynamics is reminiscence of that of $\omega = 0$, collapses and revivals are hindered by a non-regular distribution of the energy spectrum. Finally, we remark that the off-resonant condition $\omega \gg \omega_0$ becomes particularly interesting due to the emergence of a quantum phase transition [7].

III. TRAPPED-ION REALIZATION OF THE QRM IN THE DSC REGIME

In the following we analyze the impact of magnetic-field fluctuations on the realization of a QRM in the DSC regime using a trapped ion and how these fluctuations can be reduced by means of continuous DD techniques. For that, we firstly review the standard scheme to accomplish a QRM and discuss how to incorporate magnetic-field fluctuations into system dynamics. Secondly, we propose a continuous DD scheme which together with a standing wave configuration allow us to realize the QRM in this regime, as demonstrated by the numerical simulations.

We consider a typical trapped-ion scenario where the qubit is encoded using metastable states with optical transition denoted here as ω_I . In experiments performed with $^{40}\text{Ca}^+$ ions the transition is $\omega_I \approx 2\pi \times 4 \cdot 10^{14}$ Hz [17, 18]. The dynamics of the ion, confined in a trap with center-of-mass frequency ν , interacting with a set of lasers is dictated by the following Hamiltonian [13]

$$H_{\text{TI}} = \frac{\omega_I}{2}\sigma_z + \nu a^\dagger a + \sum_j \Omega_j \sigma_x \cos(\vec{k}_j \cdot \vec{x} - \omega_j t - \phi_j), \quad (2)$$

where intensity, wave vector, frequency and initial phase of each laser is denoted by Ω_j , \vec{k}_j ,

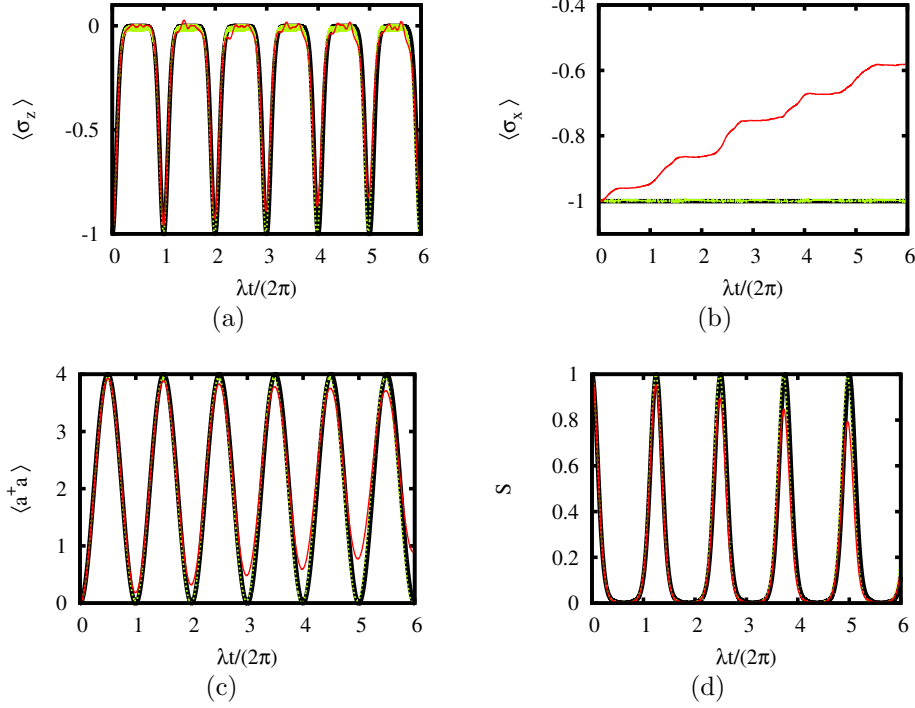


Figure 1. Trapped-ion dynamics of the QRM with $\omega = 0$ in the DSC regime where collapses and revivals emerge. The ideal dynamics is plotted with a solid black line, the unprotected realization with solid red lines and the protected scheme with dotted green lines. In (a) and (c) the simulated coupling constant is $\lambda/\omega_0 = 1$ and the initial state $|\psi(0)\rangle = |g\rangle|0\rangle$, where we show the time evolution of spin and phonon population, namely, $\langle \sigma_z \rangle$ and $\langle a^\dagger a \rangle$. In (b) and (c) the initial state $|\psi(0)\rangle = 1/\sqrt{2}(|e\rangle - |g\rangle)|0\rangle$ evolves under a simulated QRM with $\lambda = 1.25\omega_0$. In (b) $\langle \sigma_x \rangle$ is shown and the survival probability, $S(t) = |\langle \psi(0)|\psi(t)\rangle|^2$, shows that the initial state is periodically retrieved. The trapped-ion results were obtained after an ensemble average of 100 stochastic trajectories. Note the impact of magnetic-dephasing noise into the bare realization, which is accentuated at the end of the evolution after 6 ms since $\lambda = 2\pi \times 1$ kHz. See main text for further information about simulation parameters.

ω_j and ϕ_j , respectively. Considering motion along one direction, $\vec{x} = x$, the position can be written in terms of the corresponding vibrational mode, $x = x_0(a + a^\dagger)$ with $x_0 = 1/\sqrt{2m\nu}$ and m the ion mass. The coupling between the motional states and internal electronic states of the ion is quantified by the Lamb-Dicke parameter, $\eta_j = k_j x_0$. In this setup, an optical driving with $\omega_j \approx \omega_I$ can provide with a reasonably large Lamb-Dicke parameter $\eta \approx 0.04$ [18] and Rabi frequency $\Omega_j \sim 10^1 - 10^2$ kHz, while the trap frequency ν on the

range of 1 MHz.

The internal states of the ion, $|g\rangle$ and $|e\rangle$, are magnetically sensitive, as it is the case of the considered setup with $^{40}\text{Ca}^+$ ions [17, 18]. Therefore, the presence of magnetic-field fluctuations ultimately limits the coherence time. For our numerics we will take $T_2 \approx 3$ ms according to [18]. It is worth emphasizing that this is also the case for setups involving microwave-driven ions [19, 20], where $T_2 \approx 5$ ms is observed by using the hyperfine levels of the $^{171}\text{Yb}^+$ ion [19]. The effect of such magnetic-field fluctuations can be effectively captured by adding a term $\xi(t)\sigma_z/2$ to the trapped-ion Hamiltonian, such that $\xi(t)$ represents a stochastic process [21, 25–29]. Such a fluctuation is commonly described as an Orstein-Uhlenbeck process [30–32], which is a Markovian and Gaussian process exhibiting a finite-width spectral density. Thus, the time evolution of $\xi(t)$ depends on two parameters, namely, relaxation time τ and diffusion constant c . The relaxation time determines the width of the spectral density, $1/(2\pi\tau)$, and it can be estimated to be $\tau \approx 100 \mu\text{s}$ in trapped-ion experiments [28]. The diffusion constant is then determined to correctly reproduce the coherence time T_2 , which for the typical trapped-ion scenario, $T_2 \gg \tau$, simplifies to $c \approx 2/(\tau^2 T_2)$. We remark that this noise model successfully reproduces the coherence decay observed experimentally [26, 33].

The trapped-ion Hamiltonian, Eq. (2), allows to simulate the QRM in an appropriate interaction picture by driving detuned red- and blue-sidebands (denoted with the subscripts r and b , respectively), which provides with the needed JC and anti-JC interaction terms of the QRM [15, 34]. The frequencies of these two lasers are set to $\omega_{r,b} = \omega_I \mp \nu - \delta_{r,b}$, with $\delta_{r,b} \ll \nu \ll \omega_I$. Hence, $|\omega_I - \omega_{r,b}| \ll |\omega_I + \omega_{r,b}|$ which together with the condition $\eta^2 \langle (a + a^\dagger)^2 \rangle \ll 1$ (Lamb-Dicke regime), the trapped-ion Hamiltonian in an interaction picture with respect to $H = \omega_I/2\sigma_z + \nu a^\dagger a$, adopts the following form [15, 34],

$$H_{\text{TI}}^I \approx -\frac{\eta\Omega}{2} [\sigma^+ a e^{-i\delta_r t} + \sigma^+ a^\dagger e^{-i\delta_b t} + \text{H.c.}], \quad (3)$$

where $\Omega \equiv \Omega_{r,b}$ and $\eta \equiv \eta_{r,b}$ and $\phi_{r,b} = 3\pi/2$. Indeed, the previous Hamiltonian corresponds to a QRM, Eq. (1), in a rotating frame with respect to the free terms $\omega/2\sigma_z + \omega_0 a^\dagger a$, where simulated parameters of the QRM are $\omega = (\delta_b + \delta_r)/2$, $\omega_0 = (\delta_b - \delta_r)/2$ and the coupling constant $\lambda = \eta\Omega/2$. Note however that the fluctuating term, $\xi(t)\sigma_z/2$, not shown explicitly, will damage a correct realization of the QRM. It is therefore pertinent to develop a scheme to cope with this magnetic-dephasing noise.

A continuous DD scheme can be used to realize the QRM while it overcomes the aforementioned magnetic-dephasing noise, as recently proposed in [21]. However, the realization of a QRM in the DSC regime with $\omega = 0$ or $\omega \leq \omega_0$ can not be trivially achieved within the reported scheme, and demands a different strategy, as we discuss below. In general, a continuous DD method consists in providing with a new qubit dressed basis by means of an additional driving. Then, as the noise term becomes orthogonal to the new qubit basis, its effect is mostly suppressed if the corresponding qubit frequency splitting is sufficiently large such that the noise is not capable to produce transitions. In our case, the dressed basis is accomplished by an additional laser, driving a carrier interaction denoted by a subscript c , in addition to the detuned red- and blue-sidebands. Then, the resulting Hamiltonian in an interaction picture with respect to $H = \omega_I/2\sigma_z + \nu a^\dagger a$ reads

$$H_{\text{TI}}^I \approx \frac{\xi(t)}{2}\sigma_z + \frac{\Omega_c}{2}\sigma_x + \frac{\eta\Omega}{2} [\sigma^+ a e^{i\delta_r t} e^{-i(\phi_r - \pi/2)} + \sigma^+ a^\dagger e^{i\delta_b t} e^{-i(\phi_b - \pi/2)} + \text{H.c.}] . \quad (4)$$

Note that the previous Hamiltonian is achieved, first neglecting terms rotating at frequency $\omega_{c,r,b} + \omega_I$ and those at ν or higher, within the Lamb-Dicke regime. These approximations can be safely performed as in the standard case. In addition, for the carrier interaction, $\omega_c = \omega_I$, the initial phase has been already set to $\phi_c = 0$, while its corresponding Lamb-Dicke parameter η_c is not relevant, i.e. all of its sidebands are detuned by an amount $\approx |\nu|$ and are averaged out.

As a consequence of the carrier interaction, a new dressed basis can be defined according to $\Omega_c/2\sigma_x$. Then, it can be shown that the noisy term $\xi(t)\sigma_z/2$ does not produce spurious excitations in the new dressed basis if $\Omega_c > 1/(2\pi\tau)$ and provided that it is not too strong. In a trapped-ion case, with $T_2 = 3$ ms and $\tau = 100$ μ s, a Rabi frequency of the carrier $\Omega_c \sim 10^1 - 10^2$ kHz can be sufficient to overcome these fluctuations, and hence, the term $\xi(t)$ can be safely neglected [21, 26, 29]. Therefore, the QRM can be readily achieved from the previous Hamiltonian with parameters $\omega = \Omega_c$, $\omega_0 = -\delta_r = \delta_b$ and $\lambda = \eta\Omega/2$ [21]. However, the accessible parameter regime would be unnecessarily constrained to a large value for ω (for an efficient elimination of the noise). However in the DSC regime we are interested in the case where $\omega \lesssim \omega_0 \lesssim \lambda$ (i.e. ω on the order of a few kHz because, as explained above, the Rabi frequencies $\sim 10^1 - 10^2$ kHz) which corresponds to the regime where collapses and revivals emerge. Therefore, an exploration of a protected scheme of the QRM in the DSC regime is missing.

This restriction can be lifted by moving to an additional rotating frame with respect to $\Omega_D/2\sigma_x$ such that the Rabi frequency of the carrier interaction is split according to $\Omega_c = \Omega_D + \omega$. Then, the Hamiltonian becomes

$$H_{\text{TI}}^{II} \approx \frac{\omega}{2}\sigma_x + \frac{\eta\Omega}{4} [(i\sigma_x - \cos(\Omega_D t)\sigma_y + \sin(\Omega_D t)\sigma_z) \times \\ \times (ae^{i\delta_r t}e^{-i\phi_r} + a^\dagger e^{i\delta_b t}e^{-i\phi_b}) + \text{H.c.}] , \quad (5)$$

where the noisy term has been already neglected for large enough values of Ω_D , see later. Finally, choosing detunings such that $\delta_{r,b} = \Omega_D \mp \omega_0$ and initial phases $\phi_{r,b} = 0$, and performing an extra rotating-wave approximation to eliminate terms rotating at Ω_D or higher frequencies, the Hamiltonian adopts the form of a QRM in the rotating frame of $\omega_0 a^\dagger a$, i.e.

$$H_{\text{TI}}^{II} \approx \frac{\omega}{2}\sigma_x - \frac{\eta\Omega}{4}\sigma_y [ae^{-i\omega_0 t} + a^\dagger e^{i\omega_0 t}] , \quad (6)$$

where the spin basis is now rotated with respect to that of the QRM given in the Eq. (1). Note however that the previous RWA is only valid if $\Omega_D \gg \eta\Omega$, but with Ω_D still small compared to the trap frequency ν to properly resolve sidebands, $|\Omega_D \mp \omega_0| \ll \nu$, and at the same time $\Omega_{r,b} \ll |\Omega_D - \nu|$ to safely neglect detuned carrier interactions. Indeed, although the impact of the magnetic-dephasing noise is largely reduced, the QRM is not correctly achieved due to the failure of the latter RWA (i.e. the one aimed to eliminate the detuned carrier contribution). For typical parameters $\nu \sim \text{MHz}$ and $\Omega_{r,b,D} \sim 10^1 - 10^2 \text{ kHz}$, hence unwanted detuned carrier interactions become relevant.

Therefore, on top of the above commented DD scheme, we propose a standing wave configuration to eliminate the resulting spurious carrier interactions [16, 22, 23]. This consists in placing the ion at the node of two counter-propagating waves, that is, $\phi_{r,1} = \phi_{r,2} + \pi$ and $\vec{k}_{r,1} \cdot \vec{x} = -\vec{k}_{r,2} \cdot \vec{x}$ or equivalently, $\eta \equiv \eta_{r,1} = -\eta_{r,2}$. Note that two lasers are now employed to drive the detuned red-sideband, $\omega_{r,1} = \omega_{r,2} = \omega_I - \nu - \Omega_D + \omega_0$, and similarly for the blue-sideband, which finally lead to

$$H_{\text{TI}}^{II,SW} \approx \frac{\omega}{2}\sigma_x - \frac{\eta\Omega}{2}\sigma_y [ae^{-i\omega_0 t} + a^\dagger e^{i\omega_0 t}] , \quad (7)$$

where $\Omega = \Omega_{r,j} = \Omega_{b,j}$ and $\phi_{r,1} = \phi_{b,1} = 0$. In this manner we can effectively eliminate the magnetic-dephasing noise without spurious carrier contributions and, at the same time, define the parameters of the simulated QRM (note that $\omega = \Omega_c - \Omega_D$). This strategy allows

to explore a wide parameter regime including the DSC, as ω can be set now to the regime $\omega \lesssim \omega_0 \lesssim \lambda$.

The numerical simulations of trapped-ion dynamics in this work were performed assuming only the optical RWA, that is, starting from the following Hamiltonian

$$H_{\text{TI}}^I = \frac{\xi(t)}{2}\sigma_z + \sum_j \frac{\Omega_j}{2} \left[\sigma^+ e^{i\eta_j(ae^{-i\nu t} + a^\dagger e^{i\nu t})} e^{i(\omega_I - \omega_j)t} e^{-i\phi_j} + \text{H.c.} \right], \quad (8)$$

using both bare and protected scheme, as explained previously. The results are gathered in Fig. 1, together with the aimed dynamics of the ideal QRM Hamiltonian, Eq. (1). Since the trapped-ion simulations were performed including the magnetic-dephasing noise, $\xi(t)/2\sigma_z$, the results correspond to an ensemble average over 100 stochastic trajectories of the noise. The considered trapped-ion parameters are $\nu = 2\pi \times 1.5$ MHz, $\eta = 0.04$, Rabi frequencies for red- and blue-sidebands $\Omega = 2\pi \times 50$ kHz, and $\eta_c = 0.01$ and $\Omega_c = 2\pi \times 200$ kHz. In Fig. 1 we show the results corresponding to a QRM for two cases with $\omega = 0$, namely, $\lambda = \omega_0$ with initial state $|\psi(0)\rangle = |g\rangle|0\rangle$ and $\lambda = 1.25\omega_0$ (DSC regime) with $|\psi(0)\rangle = 1/\sqrt{2}(|e\rangle - |g\rangle)|0\rangle$. We recall that the initial states are referred to the spin basis of the QRM in Eq. (1), and thus, they must be rotated accordingly for the protected scheme, see Eq. (7). The results show an improvement of the protected scheme to reproduce the aimed dynamics of the QRM in the DSC regime. The simulated coupling constant results in $\lambda = \eta\Omega/2 = 2\pi \times 1$ kHz, and the simulation time goes up to 6 ms which is $2T_2$. The fidelity between the simulated and ideal dynamics at the end of the evolution exceeds 95% for the protected scheme while for the bare realization drops below 90%.

IV. SUMMARY

We propose a scheme to attain a faithful realization of the QRM in the DSC regime with a trapped ion based on continuous dynamical decoupling technique to cope with magnetic-dephasing noise. This noise constrains the coherence time, being the main source of decoherence in trapped-ion setups which involve magnetically sensitive internal states, as in experiments performed with qubits encoded in metastable states of optical ions. This noise, which features a finite spectral width, can be handled with dynamical decoupling techniques. However, the range of the simulated parameters relying on these schemes is typically narrowed, and thus, tunability is traded for noise resilience. Here, we propose a strategy to

achieve a tunable QRM and at the same time robust against magnetic-dephasing noise. We demonstrate that the proposed scheme allows to explore the DSC regime of the QRM, whose main dynamical hallmark consists in the structured dynamics of collapses and revivals.

While the standard simulation of the QRM in a trapped ion is attained by means of two lasers driving detuned red- and blue-sidebands, the proposed continuous dynamical decoupling involves the driving of a carrier interaction. This latter driving plays a fundamental role in the scheme as it defines a new dressed basis to encode the qubit and handles magnetic-dephasing noise. Nevertheless, under typical trapped-ion parameters, unwanted terms may deteriorate the correct simulation of the QRM as a consequence of an additional RWA. This obstacle can be overcome by properly setting red- and blue-sideband lasers in a standing wave configuration.

FUNDING

This work was supported by the ERC Synergy grant BioQ, the EU STREP project EQUAM and the CRC TRR21. This work was performed on the computational resource bwUniCluster funded by the Ministry of Science, Research and the Arts Baden-Württemberg and the Universities of the State of Baden-Württemberg, Germany, within the framework program bwHPC. J. C. acknowledges Universität Ulm for a Forschungsbonus.

-
- [1] I. I. Rabi, Phys. Rev. **49**, 324 (1936).
 - [2] I. I. Rabi, Phys. Rev. **51**, 652 (1937).
 - [3] G. Romero, D. Ballester, Y. M. Wang, V. Scarani, and E. Solano, Phys. Rev. Lett. **108**, 120501 (2012).
 - [4] D. Braak, Q.-H. Chen, M. T. Batchelor, and E. Solano, J. Phys. A: Math. Theor. **49**, 300301 (2016).
 - [5] E. T. Jaynes and F. W. Cummings, Proc. IEEE **51**, 89 (1963).
 - [6] D. Braak, Phys. Rev. Lett. **107**, 100401 (2011).
 - [7] M.-J. Hwang, R. Puebla, and M. B. Plenio, Phys. Rev. Lett. **115**, 180404 (2015).
 - [8] R. Puebla, M.-J. Hwang, and M. B. Plenio, Phys. Rev. A **94**, 023835 (2016).

- [9] J. Casanova, G. Romero, I. Lizuain, J. García-Ripoll, and E. Solano, *Phys. Rev. Lett.* **105**, 263603 (2010).
- [10] T. Niemczyk, F. Deppe, H. Huebl, E. P. Menzel, F. Hocke, M. J. Schwarz, J. J. Garcia-Ripoll, D. Zueco, T. Hummer, E. Solano, A. Marx, and R. Gross, *Nat. Phys.* **6**, 772 (2010).
- [11] P. Forn-Díaz, J. Lisenfeld, D. Marcos, J. J. García-Ripoll, E. Solano, C. J. P. M. Harmans, and J. E. Mooij, *Phys. Rev. Lett.* **105**, 237001 (2010).
- [12] M. Abdi, M.-J. Hwang, M. Aghtar, and M. B. Plenio, *arXiv* **1704.00638** (2017).
- [13] D. Leibfried, R. Blatt, C. Monroe, and D. Wineland, *Rev. Mod. Phys.* **75**, 281 (2003).
- [14] D. Leibfried, B. DeMarco, V. Meyer, D. Lucas, M. Barrett, J. Britton, W. M. Itano, B. Jelenković, C. Langer, T. Rosenband, and D. J. Wineland, *Nature* **422**, 412 (2003).
- [15] J. S. Pedernales, I. Lizuain, S. Felicetti, G. Romero, L. Lamata, and E. Solano, *Sci. Rep.* **5**, 15472 (2015).
- [16] R. Puebla, M.-J. Hwang, J. Casanova, and M. B. Plenio, *Phys. Rev. Lett.* **118**, 073001 (2017).
- [17] R. Gerritsma, G. Kirchmair, F. Zahringer, E. Solano, R. Blatt, and C. F. Roos, *Nature* **463**, 68 (2010).
- [18] R. Gerritsma, B. P. Lanyon, G. Kirchmair, F. Zähringer, C. Hempel, J. Casanova, J. J. García-Ripoll, E. Solano, R. Blatt, and C. F. Roos, *Phys. Rev. Lett.* **106**, 060503 (2011).
- [19] N. Timoney, I. Baumgart, M. Johanning, A. F. Varon, M. B. Plenio, A. Retzker, and C. Wunderlich, *Nature* **476**, 185 (2011).
- [20] C. Piltz, T. Sriarunothai, S. S. Ivanov, S. Wölk, and C. Wunderlich, *Sci. Adv.* **2** (2016).
- [21] R. Puebla, J. Casanova, and M. B. Plenio, *New J. Phys.* **18**, 113039 (2016).
- [22] J. I. Cirac, R. Blatt, P. Zoller, and W. D. Phillips, *Phys. Rev. A* **46**, 2668 (1992).
- [23] T. E. deLaubenfels, K. A. Burkhardt, G. Vittorini, J. T. Merrill, K. R. Brown, and J. M. Amini, *Phys. Rev. A* **92**, 061402 (2015).
- [24] D. Z. Rossatto, C. J. Villas-Bôas, M. Sanz, and E. Solano, *arXiv* **1612.03090** (2016).
- [25] A. Bermudez, P. O. Schmidt, M. B. Plenio, and A. Retzker, *Phys. Rev. A* **85**, 040302 (2012).
- [26] J.-M. Cai, B. Naydenov, R. Pfeiffer, L. P. McGuinness, K. D. Jahnke, F. Jelezko, M. B. Plenio, and A. Retzker, *New J. Phys.* **14**, 113023 (2012).
- [27] A. Lemmer, A. Bermudez, and M. B. Plenio, *New J. Phys.* **15**, 083001 (2013).
- [28] G. Mikelsons, I. Cohen, A. Retzker, and M. B. Plenio, *New J. Phys.* **17**, 053032 (2015).
- [29] R. Puebla, M.-J. Hwang, J. Casanova, and M. B. Plenio, *arXiv* **1703.10539** (2017).

- [30] G. E. Uhlenbeck and L. S. Ornstein, Phys. Rev. **36**, 823 (1930).
- [31] D. T. Gillespie, Phys. Rev. E **54**, 2084 (1996).
- [32] D. T. Gillespie, Am. J. Phys. **64**, 225 (1996).
- [33] D. J. Wineland, C. Monroe, W. M. Itano, D. Leibfried, B. E. King, and D. M. Meekhof, J. Res. Natl. Inst. Stand. Technol. **103**, 259 (1998).
- [34] J. I. Cirac, A. S. Parkins, R. Blatt, and P. Zoller, Phys. Rev. Lett. **70**, 556 (1993).